Journal of the Southeastern Association for Research in Astronomy, **4**, 7-11, 2010 July 1

THE NATURE OF MICROVARIABILITY IN BLAZAR 0716+71

Sarah M. Dhalla[1]
Department of Physics and Astronomy & The SARA Observatory, Agnes Scott College, Decatur, GA 30030

James R. Webb, Gopal Bhatta
Physics Department & The SARA Observatory, Florida Interlational University, Miami, FL 33199

Joseph T. Pollock
Department of Physics and Astronomy & Dark Sky Observatory, Appalachian State University, Boone, NC 28608

ABSTRACT

We analyze twenty-one microvariability observations of Blazar 0716+71 in order to determine the nature of the microvariations. We use the relationship between the excess RMS and time to test whether the data represents a stationary time series and we examine the distribution of fluxes to determine whether the micro variations present in the light curves are consistent with noise processes. We found that although there are characteristics of correlated noise processes with a power density fluctuation spectrum of 1/f in the data, we show that we do not have an adequate number of observations to verify that all of the variations we see can be attributed to a Gaussian noise process and therefore rule out any deterministic signals in the data.

Subject headings: (galaxies:) BL Lacertae objects: general

1. INTRODUCTION

Quasars are a subset of active galactic nuclei (AGN) that are thought to be extremely luminous, compact, and distant objects. Current quasar models assume that these objects are powered by rotating super massive black holes which are believed to have masses on the order of 10^6-10^9 solar masses. Accretion disks formed by the large amount of in-falling material supply mass and strong magnetic fields, some of which are ejected into powerful plasma-carrying relativistic jets oriented perpendicular to the disk. The Blazar category consists of a subset of quasars which exhibits rapid, high-amplitude optical flares, and BL Lac type objects. The basic Blazar models assume that their relativistic jets are directed along the line of sight to Earth. These strong Blazar jets are highly collimated by large scale magnetic fields, and are believed to be the source of the optical variations we observe in Blazars.

Blazar variability is usually divided into three types: long-term variability, short-term variability, and microvariability (Gupta et al. 2008). Long term variability occurs on timescales of several years whereas short-term variations occur on timescales of months to weeks. While long term and short term variations are likely directly related to major shocks launched into the jets, the microvariation which are characterized by brightness changes of a few tenths of a magnitude over hours to minutes and fluctuate on timescales of a few minutes to hours, are more likely correlated with inhomogenieties and turbulence in the jet emission region. Most Blazars show microvariability, but only intermittently. The active Blazar 0716+71 was chosen for this study since its duty cycle, the amount of time that the object is varying compared to the amount of time it has been observed, is 90.3% (Webb 2007). This is the highest duty cycle we have observed on our sample.

Downs et al. (2003) studied a set of microvariability observations of 0716+71 using Discrete Fourier Transform (DFT) analysis. Seven of these microvariability events showed weak evidence of a common timescale on the order of 2.2 ± 0.8 hr in the observers frame. These results were inconclusive and it was possible the timescales were spurious based on the short length of the light curves. Azarnia et al. (2005) re-examined these observations using the DFT in log-log space in order to see if the DFTs were better represented as noise processes. Once the high frequency white noise component was trimmed off, the DFT resembled $1/f$ noise with the exception of a few weak features. Humrickhouse et al. (2007) also analyzed these observations, this time using Wavelets, but once again the results were inconclusive due to the limited length of the data sets and the fact that none of the periods identified were repeated in every observation. Since the light curves we have collected have limited temporal coverage, and the DFT can only be applied to individual continuous segments, it has proved to be limited in its effectiveness in finding evidence of deterministic timescales (Humrickhouse et al. 2007). As new data became available, the DFT and Wavelet analysis were run on these light curves and in each case failed to yield repeatable periods.

In many cases when only a small number of light curves of inadequate length are available, statistical measurements such as the variance and mean can be used to determine the noise content of the variations when several non-contiguous observations are added together (Vaughan et al. 2003). If the underlying process causing

Electronic address: sdhalla@agnesscott.edu, webbj@fiu.edu, gopal.bhatta@fiu.edu, pollockjt@appstate.edu
[1] Southeastern Association for Research in Astronomy (SARA) NSF-REU Summer Intern.

the microvariability is a stationary noise process, then each light curve would exhibit the same statistical characteristics. Understanding the statistical characteristics of the noise is the first step to understanding the underlying physical processes causing the variations. Noise is often found in many processes in nature and need not be entirely uncorrelated on all timescales. The power spectrum exhibited by a particular system characterizes the type of noise. The DFT frequency and power of a signal are related in the following way:

$$P = 1/f^{\beta} \quad (1)$$

(where β is the spectral slope of the Power Density Spectrum (PDS)). random noise, also known as white noise, is characterized by a spectral slope of zero. Statistical error and thermal noise of the imaging device are examples of white noise processes. Flicker noise, characterized by a β of 1 can be seen in stochastic processes in nature, including music. Brownian motion is a third type of noise, also called red noise, which is characterized by a spectral slope of 2. In Brownian motion or random walking in solutions, each step is dependent on the previous step(Azarnia et al. 2005). If in fact the microvariations seen in Blazar light curves are due to a stationary noise process, each of our microvariability light curves would represent one realization of the underlying stochastic process. Statistical descriptions of a noise process has been used to analyze the X-ray observations of three AGN by Uttley et al. (2001), and they showed that a linear relationship existed between the RMS variability and the mean flux. Cyg X-1 also showed a linear relationship in x-ray variations between flux and RMS (Uttley et al. 2005), while Superina et al. (2008) found that this relationship is also present in γ-ray light curves as well. The objective of this study is to analyze the optical microvariations of 0716+71 using the statistical procedures described in (Vaughan et al. 2003). We describe the observations in section 2, and the then describe our analysis procedures in section 3. Section 4 presents the results and we discuss the implication in section 5.

2. OBSERVATIONS

The observations analyzed here were obtained as a part of a continuous monitoring program carried out at the Southeastern Association for research in Astronomy (SARA) Observatory at Kitt Peak National Observatory located near Tucson, Arizona. Most of the images used in this study were taken through the SARA 0.9 m $f/7$ Ritchey-Chrtien telescope equipped with several CCD cameras including the an Apogee AP7 camera containing a SiTE chip and the Apogee U42. Additional data were taken by J. Pollock at the Appalachian State University Dark Sky Observatory (DSO) in the Blue Ridge Mountains using a 0.81m $f/13$ Cassegrain telescope with a Photometrics CH250 camera with a 1024 $\times$ 1024 TK1024AB1 chip. All images were reduced using the MIRA Pro software and were corrected for bias, dark current and flat field. Each image was cosmic ray corrected to improve accuracy in photometry. Aperture photometry was done in MIRA using three comparison stars from the standard WEBT sequence. The measured magnitudes were then imported into an excel spreadsheet for analysis and display. The presence of microvariability was determined for each light curve using the statistical method described by Howell et al. (1988), and only those observations that had high signal-to-noise, yielded positive for micro-variations, and were of long enough duration to be statistically significant were used in this study. The data set studied here includes twenty-one light curves, thirteen more than previous studies (Humrickhouse et al. 2007).

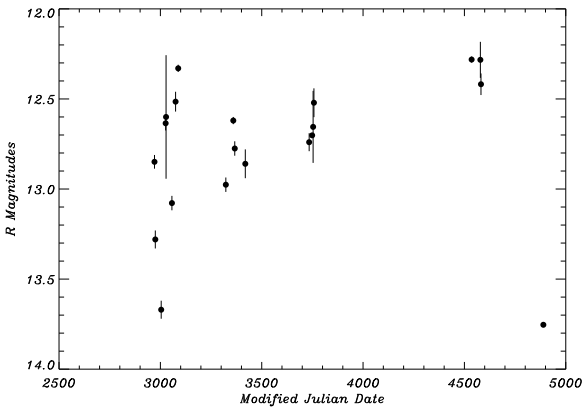

FIG. 1.— The long term light curve that resulted from over of six years of microvariability monitoring of 0716 + 71. Each data point represents between 200 and 800 individual CCD images. The bars indicate the range of variability during the course of the microvariability observation. The errors are much smaller than the symbol size for each point.

3. ANALYSIS

The six year long-term light curve showing the flux levels of each individual microvariability observation can be seen in Figure 1. Note that the triangles represent observations in which microvariability was detected, squares represent observations in which no microvariability was detected, and the filled points represent monitoring observations. Note that the data cover the entire range of short-term variations historically seen in 0716+71, thus we have a reasonable sampling of its variability characteristics. It has been shown (Webb 2007) that the presence of microvariations does not correlate with the short term brightness level.

We converted the magnitudes to flux (Janskys) using the standard conversion formulas and the measured reddening values. The flux curves were plotted for each of the observations. Figure 2 is an example of a microvariability flux curve for a specific night. Each point in Figure 2 represents a single CCD image. Following Vaughan et al. (2003), we binned each microvariability light curve into bins that were thirty minutes long. Each bin was an average of all the data points within those thirty minutes. For example, assuming that the data set begins at UT 2:00:00, then the first bin would contain all data points between UT 2:00:00 and UT 2:30:00. The next bin would begin at UT 2:30:01 or whatever time the next observation was taken and so forth. Data sets with less than twenty observations per bin were excluded to ensure that each bin had at least twenty data points for statistical accuracy. In some cases data points towards the end of the data set were excluded because the bin did not last thirty minutes. The average flux and average RMS was then calculated for each bin. The RMS is

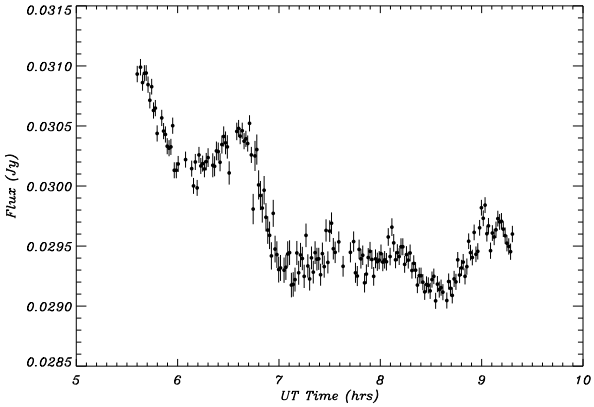

FIG. 2.— A typical microvariability light curve of 0716+71. This example curve is from 01/22/2006.

defined in equation two.

$$x_{\rm RMS} = \sqrt{\frac{1}{N}\sum_{i=1}^{N}(x_i - \bar{x})^2} \qquad (2)$$

We then treated each individual light curve as an individual bin, or "super bin", to calculate the excess RMS of the variations. In this second order binning procedure, all the bins in each data set were

averaged producing super bins, which resulted in twenty-one super bins (one for each microvariability observation) Although each super bin was not the same length, each super bin did have at least 97 observations. Table 1 lists the observations analyzed in this research and the relevant calculated values for excess RMS as described above. The first column shows the date the observation was made, while the second column shows the average flux observed during that observation. Note the observations were not necessarily the same duration, but each one showed significant microvariability during the observation. The excess RMS is listed in the third column along with the propagated errors in the final two columns. Errors for data containing (*) were estimated and ranged between 0.0001-0.0003 since the actual photometric errors were not available.

TABLE 1
AVERAGE FLUX AND EXCESS RMS OF OBSERVATIONS

Date[a] (UT)	Ave. Flux (mJy)	Excess RMS	σ_+	σ_-
2003 Dec 1*	14.72	0.13	0.10	0.10
2003 Dec 29*	10.28	0.07	0.10	0.10
2004 Jan 11*	26.59	0.14	0.20	0.20
2004 Jan 21*	26.62	0.14	0.30	0.30
2004 Jan 23*	27.68	0.44	0.30	0.30
2004 Feb 21*	17.80	0.15	0.10	0.10
2004 Mar 3*	29.95	0.18	0.20	0.20
2004 Mar 23	35.34	0.17	0.01	0.09
2004 Nov 13*	19.63	0.09	0.20	0.20
2004 Dec 12*	23.50	0.11	0.20	0.02
2005 Feb 17*	21.72	0.17	0.10	0.10
2005 Dec 12	24.24	0.43	0.07	0.07
2006 Jan 13	25.13	0.12	0.05	0.05
2006 Jan 18	26.36	0.20	0.03	0.03
2006 Jan 22	29.73	0.20	0.08	0.08
2006 Jan 28	14.08	0.24	0.05	0.05
2008 Feb 18	27.10	0.13	0.07	0.07
2008 Mar 05	29.42	0.28	0.11	1.15
2008 Mar 10	28.66	0.15	0.03	0.03
2008 Apr 22	36.86	0.33	0.11	0.11
2008 Apr 25	32.76	0.31	0.11	0.11

[a] Errors for data containing (*) were estimated and ranged between 0.1-0.3 since the actual photometric errors were not available.

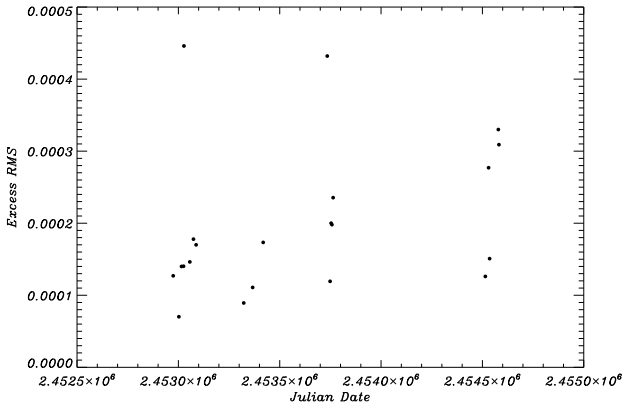

FIG. 3.— The Excess RMS is plotted versus time. If the time series is stationary and we have ample sampling, the points should be consistent with a straight line.

4. RESULTS

4.1. *Statistical Results*

According to Vaughan et al. (2003), a stationary process should exhibit a linear relationship when the excess RMS and the time are plotted together. Figure 3 shows a plot of the excess RMS versus time. Although the variations are large, it is not inconsistent with a stationary time series because of the relatively large error bars. Of the two major outliers, only one is more than 3 sigma away.

We then plotted the excess RMS versus the flux in Figure 4, taking into account the errors. If the variations are due solely to noise processes, we once again expected to see a plot consistent with a line. It is obvious from Figure 4 that the significance of the line fit is weak (R^2 =0.1587) with some major outliers present.

The results shown in Figures 3 and 4 are inconclusive with rather large uncertainties. A final approach with this data is to plot a histogram of the number of times the flux achieves a particular flux level. The resulting distribution is shown in Figure 5. This plot was made by dividing the fluxes up into 10 flux bins and simply counting the number of CCD images that recorded a flux level within that particular bin. For a linear noise process, this plot should yield a Gaussian distribution and for a multiplicative noise process, this process should yield a lognormal distribution. The lack of normal or log normal distributions in Figure 6 is not indicative of a pure noise process.

4.2. *Simulation Results*

In order to assess the effectiveness of the methods used here with our data, we used a Fourier Filtering spectral synthesis method (Voss 1988) programmed in IDL to compute realizations of the noise process with a partic-

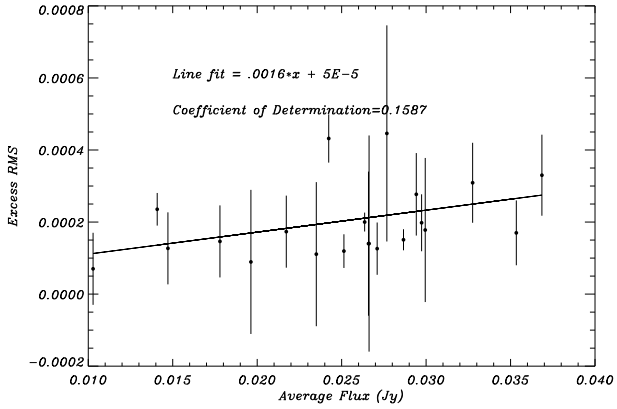

FIG. 4.— Excess RMS vs Average Flux values of each individual light curve

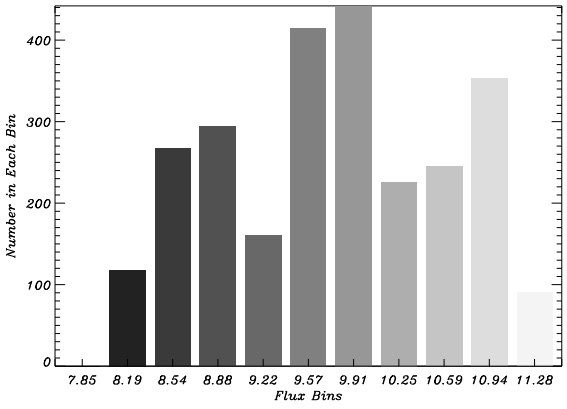

FIG. 5.— Frequency Distribution of observed flux values

ular DFT slope. The output of the program is a light curve of specified number of data points whose variations are distributed according to the input power law spectrum. We wrote specialized IDL routines to statistically analyze the simulated light curves as described in section 3. We ran 10,000 simulations with the exact same number of data points as our data, and using the same PSD of the variations as determined by DFT analysis of Azarnia et al. (2005). We found that the RMS excess versus time showed similar characteristics to our data, e.g. showing a weak linear relationship indicating that they are marginally stationary. We also found that the flux distributions showed that 15% of the simulated data sets were reasonably fit by Gaussians (half of them looked more lognormal), chisquare significance of 95%, while 85% were decidedly non-Gaussian and similar in form to our actual data. We also simulated larger data sets and found that data sets with 10,000 or more points the distribution was more consistent with a guassian distribution indicating that we are still data limited in spite of accumulated data over 6 years of microvariability study.

5. DISCUSSION

Although stationary stochastic processes may show many different realizations (light curves), but the statistical properties of these light curves (mean and variance) should not change with time Vaughan et al. (2003). The previous analysis of Azarnia et al. (2005) showed that the DFT of the fluctuations were consistent with a power law PSD with slope of -1.14 ± 0.12. The remaining features in the spectra were examined by Humrickhouse et al. (2007) who, using wavelet analysis, found that the features were not constant throughout all of the microvariability curves, thus could be interpreted as individual excursions from the power law distribution. Using the statistical analysis techniques described here, we further explored the nature of the noise component and found that the observed variations are at least consistent with noise processes. However, since there are several outliers in Figures 3 and 4, and simulations indicate that we still do not have enough data to prove the existence of strictly noise-like variations, there remains a possibility that some of the variations are deterministic in nature.

Assuming the microvariations are primarily the result of stochastic noise processes in the relativistic jets, we address the possible sources of these variations in Blazar jet models. Benford et al. (1980) proposed a turbulence model for relativistic jets in Quasars and extragalactic radio source jets. In this model, turbulence in the jets caused variations in the morphology of the jets and also in the luminosity. Although his paper focussed on the morphological variations in the radio jet caused by turbulent processes, we would expect turbulence in the inner jet regions where the optical flux emerges. The details of the noise spectrum might constrain the turbulent processes in the jet and allow us to determine physical properties in the turbulent plasma. For instance, turbulent media releases most of its energy at the smallest length scales, similar to the Kolomogrov scale in non-relativistic turbulence. Identification of the smallest timescale of variability in the microvariability curves, and the PDS of the noise would help constrain the densities and velocities in the turbulent medium. Lehto (1989) discusses possible processes to explain $1/f$ type variability in AGN. He uses multiple shot noise processes with each pulse having a particular decay time to derive a $1/f$ noise spectrum. Although he primarily applies his model to accretion phenomena, it could just as easily be used to describe processes in a relativistic jet. Each cell in the jet material would have a specific pulse height and decay time that properly convolved yields a power-law noise spectrum.

6. CONCLUSION

We analyzed twenty-one microvariability observations of blazar 0716+71. We conclude that the variations seen in the microvariability curves are marginally consistent with power law distributed noise. However, several statistical outliers prevent us from conclusively establishing the nature of the microvariations. We used simulations to show that we are still limited by the length and number of observations and we need more data to confirm that there is only noise and no deterministic component present in the data.

7. ACKNOWLEDGEMENTS

This project was funded by a partnership between the National Science Foundation (NSF AST-0552798), Research Experiences for Undergraduates (REU),and the Department of Defense (DoD) ASSURE (Awards to

Stimulate and Support Undergraduate Research Experiences) programs. We would like to acknowledge a very interesting and stimulating discussion with Dr. Steve Shore of the University of Piza about noise processes and shock propagation in jets.

Facilities: Florida International University, KPNO (SARA).

REFERENCES

Azarnia, G.M. et al., 2005, I.A.P.P.P. Comm., 101, 1
Benford, G. et al., 1980, ApJ, 241, 98
Downs, C., et al.,SARA NSF REU final meeting, Valdosta State University, Aug 2004
Gupta, A.C., et al. 2008, AJ, 135, 1384
Howell, S. B., Mitchell, K. J., & Warnock III, A. 1988, AJ, 95, 247
Humrickhouse, C. et al. 2007, JSARA, 2, 23
Lehto, H.J., ESA SP-296, November 1989
Superina, G., et al. 2008, PoS, 2008, 66
Uttley, P. et al. 2001, MNRAS, 323, L26
Uttley, P. et al. 2005, MNRAS, 359, 345
Vaughan, S. et al. 2003, MNRAS, 345, 1271
Voss, R.F., Fractals in Nature from The Science of Fractal Images, Peitgen, Saupe editors, Springer-verlag 1988
Webb, J.R., 2007, BAAS, 210, 0202